Schwann cells had lost their surface galC (Fig. 1). Addition of $10^{-3}M$ 8-bromo cyclic AMP or $10^{-3}M$ dibutyryl cyclic AMP on day 4 of culture resulted in the reappearance, within the next 3 days, of Schwann cells bearing surface galC. The proportion of galC-bearing Schwann cells peaked 5 days after addition of 8-bromo cyclic AMP or dibutyryl cyclic AMP (Fig. 1). Schwann cells positive for surface galC were not detected when concentrations of the cyclic AMP derivatives were less than $5 \times 10^{-4}M$. 8-Bromo cyclic AMP at $10^{-3}M$ was a more potent inducer of surface galC than was dibutyryl cyclic AMP at the same concentration. The high concentrations of the cyclic AMP analogs necessary to produce this effect may be attributable, at least in part, to relatively poor penetration of the analogs (*7*) into the Schwann cells. Larger concentrations of these agents did not increase the proportion of galC-positive cells (Table 1) and, in fact, treatment with $10^{-2}M$ dibutyryl cyclic AMP did not yield galC-positive Schwann cells. Because a maximum of 48 percent of the Schwann cells became positive for surface galC after treatment with the cyclic AMP derivatives, we cannot exclude the possibility that the cultures contained two populations of Schwann cells that appeared to be morphologically identical but that differed in their capacity to respond to such treatment.

To test whether induction of galC by dibutyryl cyclic AMP was attributable to butyrate, we cultured the cells in the presence of $10^{-3}M$ butyrate. No cells with surface galC appeared in such cultures during the ensuing week. Nor did treatment with $5 \times 10^{-3}M$ butyrate induce the appearance of galC-positive cells (Table 1).

Binding of antibodies to galC on the surface of cells treated with 8-bromo cyclic AMP and dibutyryl cyclic AMP showed a granulofloccular distribution, and the perinuclear region was more prominently fluorescent than the peripheral processes (Fig. 2). This distribution of binding of antibodies to galC resembled that observed in freshly isolated galC-positive Schwann cells.

In order to determine whether the appearance of galC on the surface of the treated Schwann cells was due solely to redistribution of this lipid from the interior of the cells or whether these cyclic AMP derivatives also stimulated Schwann cells to synthesize this myelin lipid, we incubated treated and control Schwann cells with D-[1-^{3}H]galactose. Incorporation of ^{3}H into galC by the 8-bromo cyclic AMP– and dibutyryl cyclic AMP–treated cultures was 15 times greater than that in the controls (Table 2).

These results indicate that derivatives of cyclic AMP can induce Schwann cells to synthesize galC and to express this myelin component on their surface; they also strengthen the possibility that cyclic AMP is a messenger involved in the process by which axons signal Schwann cells to synthesize myelin (*8*).

GEN SOBUE
DAVID PLEASURE
Children's Hospital of Philadelphia and *Departments of Neurology* and *Pediatrics, University of Pennsylvania, Philadelphia 19104*

References and Notes

1. H. J. Weinberg and P. S. Spencer, *Brain Res.* **113**, 363 (1976); A. J. Aguayo, L. Charron, G. M. Bray, *J. Neurocytol.* **5**, 565 (1976); R. P. Bunge and M. B. Bunge, *J. Cell Biol.* **78**, 943 (1978).
2. S. Strickland, K. K. Smith, K. R. Marotti, *Cell* **21**, 347 (1980); T. J. Chaplinski and J. E. Niedel, *J. Clin. Invest.* **70**, 953 (1982); B. E. Carlin, M. E. Durkin, B. Bender, R. Jaffe, A. E. Chung, *J. Biol. Chem.* **258**, 7729 ((1983)
3. A. K. McMorris, *J. Neurochem.* **41**, 506 (1983); *Proc. Natl. Acad. Sci. U.S.A.* **74**, 4501 (1977).
4. M. C. Raff *et al.*, *Nature (London)* **274**, 913 (1978); M. C. Raff, K. Fields, S. Hakomori, R. Mirsky, R. Pruss, J. Winter, *Brain Res.* **174**, 283 (1979); R. P. Lisak, R. M. Pruss, P. G. E. Kennedy, O. Abramsky, D. E. Pleasure, D. H. Silberberg, *Neurosci. Lett.* **17**, 119 (1980).
5. A. Mirsky, J. Winter, E. R. Abney, R. M. Pruss, J. Gavriolovic, M. C. Raff, *J. Cell Biol.* **84**, 483 (1980).
6. B. Q. Kreider, A. Messing, H. Doan, S. U. Kim, R. P. Lisak, D. E. Pleasure, *Brain Res.* **207**, 433 (1981).
7. D. K. Granner, L. Sellers, A. Lee, C. Butters, L. Kutina, *Arch. Biochem. Biophys.* **169**, 601 (1975); J. Singh and F. W. Flitney, *Biochem. Pharmacol.* **30**, 1475 (1981).
8. Dibutyryl cyclic AMP has been reported to promote the proliferation of cultured rat Schwann cells [M. C. Raff, A. Hornby-Smith, J. P. Brockes, *Nature (London)* **273**, 672 (1978)]. We examined the effects of $10^{-7}M$ to $10^{-2}M$ 8-bromo cyclic AMP and dibutyryl cyclic AMP on incorporation of tritiated thymidine into the trichloroacetic acid–insoluble fraction of rat Schwann cell cultures. These cyclic AMP derivatives increased the uptake of tritiated thymidine by Schwann cells; maximum stimulation was observed at $10^{-4}M$ to $5 \times 10^{-4}M$ concentrations with either 8-bromo or dibutyryl cyclic AMP. However, at $10^{-3}M$ 8-bromo cyclic AMP or dibutyryl cyclic AMP, the optimum concentration for induction of surface galC, the incorporation of tritiated thymidine was slightly less than that in untreated control cultures.
9. S. L. Miller, J. A. Benjamins, P. Morell, *J. Biol. Chem.* **252**, 4025 (1977); A. McMorris, S. L. Miller, D. Pleasure, O. Abramsky, *Exp. Cell Res.* **133**, 395 (1981).
10. This work was supported by grants from the Muscular Dystrophy Association, National Multiple Sclerosis Society, National Neurofibromatosis Foundation, and National Institutes of Health (HD08536, NS08075, NS11037). G.S. is a research postdoctoral fellow of the Muscular Dystrophy Association.

7 November 1983; accepted 26 January 1984

A New Charge-Mosaic Membrane from a Multiblock Copolymer

Abstract. *A charge-mosaic membrane was prepared from a pentablock copolymer of the BABCB type by selectively introducing anion and cation exchange groups into the microseparated phases. The three-layer lamellar structure of the starting pentablock copolymer film was not disturbed by the modifications. The membrane obtained was highly permeable only to sodium chloride in mixed aqueous solutions of sodium chloride and organic species of low molecular weight, such as sucrose. Marked* pH*-dependent permeabilities were also observed for amino acids.*

Charge-mosaic membranes, which are composed of cation- and anion-permeable domains, have been of continuing interest since being proposed by Sollner (*1*) in connection with biological phenomena. Theories concerning their structure have been presented (*2*); in practice, their transport properties, such as high permeability for salts, piezodialysis, or negative osmosis, have been observed in membranes prepared in various ways (*3, 4*). Early methods for preparing charge-mosaic membranes were reviewed by Leitz (*4*). However, those membranes were fragile and lacked well-defined domain structures.

If the microphase separation phenomenon of block copolymers (*5*) can be used to prepare charge-mosaic membranes, resulting membranes should have many pairs of anion and cation exchange microdomains. To prevent the formation of a poly-ion complex in such membranes, a triblock copolymer of the ABC type—composed of terminal polymer blocks A and C into which cation and anion exchange groups, respectively, are introducible and a middle polymer block B into which neither ion exchange group is introducible—should be used. This type of triblock copolymer forms a three-layer lamellar structure with the repeating unit -A-B-C-B-, where A, B, and C represent the domains consisting of their polymers (*6–8*). However, our early trial with triblock copolymers of the ABC type revealed that the lamellar structures do not withstand chemical treatments for introducing ion exchange groups, even if the neutral B domains are cross-linked.

Anionic polymerization allowed us to prepare a pentablock copolymer of the BABCB type that can generate the same three-layer lamellar structure as the ABC triblock copolymer (*8, 9*). But, in

the pentablock copolymer, the chain ends of each A and C block can be anchored to the adjacent B domains. Cross-linking the B domains, therefore, causes the structure to become rigid.

The pentablock copolymer of the BABCB type was prepared in a sealed glass apparatus at reduced pressure (10^{-6} torr); isoprene (6.5 g), styrene (9.6 g), isoprene (6.5 g), 4-vinylbenzyldimethylamine (4-VBDMA) (13.9 g), and isoprene (6.2 g) were polymerized stepwise with *sec*-butyllithium (1.08×10^{-4} mole) as the initiator and benzene (approximately 1000 ml) the solvent. The monomers and the solvent were purified (*7*) before the polymerization techniques (*10, 11*) were applied. The poly(4-VBDMA) and polystyrene blocks can be easily quaternized and sulfonated, respectively, and the polyisoprene block can be easily cross-linked. The osmometrically determined molecular weight M_n of the finally obtained polymer was 3.8×10^5 g/mole, which is in good agreement with the value calculated from the amounts of the monomers and the initiator. The M_n values of BA, BAB, and BABC precursors, taken out at the respective polymerization steps, were also close to their calculated values. Moreover, the final polymer and the precursors each showed a single, narrow peak when subjected to gel permeation chromatography, and no undesirable shoulder was observed in its ultracentrifugal sedimentation pattern. The block copolymerization thus proceeded successfully.

The film (about 50 μm thick) was cast on mercury from a benzene solution of the pentablock copolymer by evaporating benzene very slowly at 25°C in a stream of dry air. Benzene is a good solvent for the three component polymers. Electron micrographs of the film stained with osmium tetroxide (Fig. 1A) reveal a three-layer lamellar structure with a repeating unit, -S-I-A-I-, where S represnts the polystyrene domain, I the polyisoprene domain, and A the poly(4-VBDMA) domain. Any fraction of the film showed almost the same structure as this, implying the continuities of S, A, and I lamellae over large distances.

Cation and anion exchange groups were introduced into the film as follows. First, nitrogen atoms in the poly(4-VBDMA) parts were quaternized by treating the film with methyl iodide vapor for about 20 hours at 25°C at a pressure about 1/3 that of the saturated vapor. Next, the isoprenes were cross-linked with sulfur monochloride dissolved in nitromethane (20 ml per 100 ml). The reaction time was about 3 hours at 25°C. The infrared absorption bands due to the double bonds in polyisoprene almost disappeared after cross-linking. Sulfonation of the polystyrene parts was performed with chlorosulfonic acid dissolved in chloroform (2 ml per 100 ml; 15 minutes, 25°C).

The titrimetrically determined anion and cation exchange capacities of the finally obtained membrane were 0.91 and 1.2 meq per gram of dry membrane, respectively. They were nearly equal to each other and close to their calculated values. The cation transport number determined for KCl by measuring the concentration membrane potential was 0.57. It is close to 0.50, the ideal value for charge-mosaic membranes. The membrane showed negative osmosis for an aqueous solution of KCl (as is theoretically expected for a charge-mosaic membrane), and the reflection coefficient was estimated to be about −1.0 (*12*). An electron micrograph of the membrane stained with a saturated solution of stannous chloride reveals a three-layer lamellar structure with a repeating unit, $-S^-$-I-A^+-I- (Fig. 1B); the initial microstructure appeared scarcely damaged during the chemical treatments. Here S^- represents the sulfonated polystyrene domain, I the cross-linked polyisoprene domain, and A^+ the quaternized poly(4-VBDMA) domain.

The charge-mosaic membrane obtained was tested with dialytic separations. The dialysis cell consisted of two compartments (20 cm^3 each) divided by the membrane. The dialysand compartment (I) was filled with an aqueous solution of NaCl and either sucrose or one of the amino acids. For the solutions of NaCl with sucrose, the initial concentrations c_I (0) in the dialysand were both 0.1 mole/liter. For the solutions of NaCl with amino acid, the values of c_I (0) were both 2×10^{-2} mole/liter. The dialysate compartment (II) was filled with an aqueous solution of NaCl with an initial concentration of 2×10^{-4} mole/liter. The *p*H in the dialysand and dialysate was adjusted with concentrated solutions of HCl and NaOH. The effective area of the membrane was 0.78 cm^2. Twenty hours was allowed for dialysis.

Concentration ratios c_{II}/c_I (0) for Na^+ and the organic species were plotted against *p*H (Fig. 2). For the solutions of NaCl with sucrose, at every *p*H, Na^+ concentration in the dialysate increased and became close to that in the dialysand, whereas the sucrose concentration in the dialysate was low even after 20 hours of dialysis. Thus, the transport rate of NaCl through the membrane was much higher than that of sucrose.

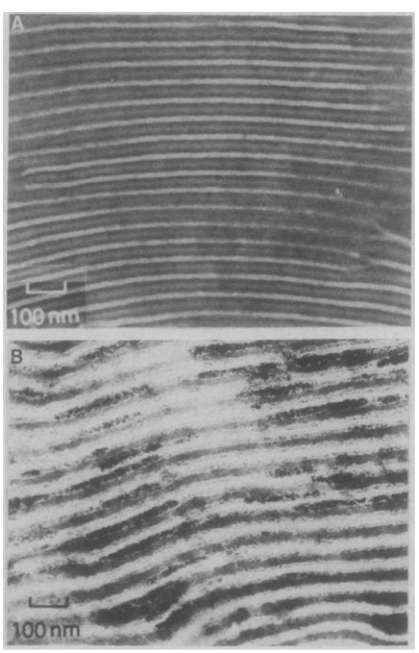

Fig. 1. (A) Electron micrograph of a pentablock copolymer, stained with OsO_4. The light, gray, and dark regions are the polystyrene, poly(4-VBDMA), and polyisoprene domains, respectively. (B) Electron micrograph of the charge-mosaic membrane prepared from a pentablock copolymer and stained with $SnCl_2$. The light and dark regions are the quaternized poly(4-VBDMA) and sulfonated polystyrene domains, respectively, and their intermediary region is the cross-linked polyisoprene domain.

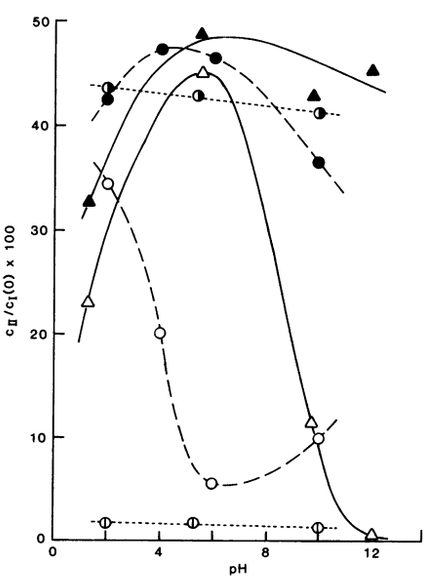

Fig. 2. Dialysis of mixed aqueous solutions of NaCl and organic species at various *p*H. The ordinate represents the ratio of the concentration of each solute in the dialysate compartment after 20 hours of dialysis (c_{II}) to the initial concentration of the solute in the dialysand compartment [$c_I(0)$]. Symbols: ◑, Na^+, and ⦶, sucrose, in their mixed solutions; ▲, Na^+, and △, lysine, in their mixed solutions; ●, Na^+, and ○, glycine, in their mixed solutions.

For the solutions of NaCl plus glycine (isoelectric point, *p*H 5.97) and NaCl plus lysine (*p*H 9.70), the permeation rates of the amino acids were low at their isoelectric points (at which amino acids are neutral), but the rates of positively charged amino acids were as high as those of Na^+. The permeation rate of Na^+ was also dependent on *p*H but less than the permeation rates of amino acids.

Our charge-mosaic membrane can be envisioned as a model of a biological membrane in that it has a mosaic structure composed of small cation and anion domains. Thus, the charge-mosaic membrane may be useful not only as a selective membrane for organic species of low molecular weight and inorganic salts but also for some biomedical materials.

TERUO FUJIMOTO
KOJI OHKOSHI
Department of Materials Science and Technology, Technological University of Nagaoka, Kamitomioka-cho, Nagaoka 949-54, Japan
YOSHIYUKI MIYAKI
Central Research Laboratory, Toyo Soda Manufacturing Company, Shin-Nanyo, Yamaguchi 746, Japan
MITSURU NAGASAWA
Department of Synthetic Chemistry, Nagoya University, Chikusa-ku, Nagoya 464, Japan

References and Notes

1. K. Sollner, *Biochem. Z.* **244**, 370 (1932).
2. R. Neihof and K. Sollner, *J. Phys. Colloid Chem.* **54**, 157 (1950); *J. Gen. Physiol.* **38**, 613 (1955); O. Kedem and A. Katchalsky, *Trans. Faraday Soc.* **59**, 1918 (1963); *ibid.*, p. 1931; *ibid.*, p. 1941; J. N. Weinstein, B. J. Bunow, S. R. Caplan, *Desalination* **11**, 341 (1972); F. B. Leitz, *ibid.* **13**, 373 (1973).
3. J. N. Weinstein and S. R. Caplan, *Science* **161**, 70 (1968); *ibid.* **169**, 296 (1970).
4. F. B. Leitz, in *Membrane Separation Processes*, P. Meares, Ed. (Elsevier, Amsterdam, 1974), p. 261.
5. G. E. Molau, in *Block Polymers*, S. L. Aggarwal, Ed. (Plenum, New York, 1970), p. 79.
6. K. Arai, T. Kotaka, Y. Kitano, K. Yoshimura, *Macromolecules* **13**, 1670 (1980).
7. Y. Matsushita, H. Choshi, T. Fujimoto, M. Nagasawa, *ibid.*, p. 1053.
8. H. Funabashi *et al.*, *ibid.* **16**, 1 (1983).
9. Y. Isono *et al.*, *ibid.*, p. 5.
10. T. Fujimoto and M. Nagasawa, *Polym. J.* **7**, 397 (1975).
11. T. Fujimoto *et al.*, *Macromolecules* **11**, 673 (1978).
12. The reflection coefficient σ_m was calculated from volume flows J_v measured under osmotic pressure difference $\Delta\pi$ with aqueous solutions of sucrose and under chemical potential difference $\Delta\mu_s^c$ of KCl across the membrane by use of the equation

$$J_v = L_p^m(\Delta p - \Delta\pi) + c_s L_p^m(1 - \sigma_m)\Delta\mu_s^c$$

L_p^m is filtration coefficient, Δp is hydrostatic pressure difference, and c_s is logarithmic average salt concentration.
13. We thank H. Hasegawa for taking the electron micrographs, M. Tasaka for measuring membrane potential, and M. Fukuda and A. Akimoto for their continuing interest and encouragement. Supported in part by a grant in aid for scientific research from the Ministry of Education, Japan (Special Project Research, Multiphase Biomedical Materials).

18 October 1983; accepted 30 January 1984

Carnivorous Mushrooms

Abstract. *Ten species of gilled fungi, including the oyster mushroom (*Pleurotus ostreatus*), have been shown to attack and consume nematodes. It is suggested that these wood-decay fungi utilize the nutrients in their prey to supplement the low levels of nitrogen available in wood. This mode of nutrition is similar in principle to that of carnivorous higher plants.*

Approximately 450 species of flowering plants are known to capture and digest small animal prey (*1*). These carnivorous plants, including sundews, pitcher plants, and the venus flytrap, derive a significant proportion of their nitrogen nutrition through their carnivorous habit (*1*). This ability to utilize a unique source of nutrients has enabled such plants to thrive in nitrogen-poor environments such as acid bogs.

Fungi that prey on small animals are also well known, including some 150 species that attack nematodes (*2*). Many of these fungi produce specialized trapping devices such as adhesive knobs, nets, or constricting rings to capture their victims, which are subsequently colonized and digested. Among the predatory fungi are nine species of *Nematoctonus* (Hyphomycetes), in which adhesive secretory cells are produced on either hyphae or asexual spores (conidia). Conidial fungi are given "form names" which apply only to their conidial state. If a sexual stage of a conidial fungus is discovered, the fungus is then given the name reflecting its classification in the system devised for the sexually reproducing fungi. The form genus *Nematoctonus* Drechsler (*3*) is distinguished from all other nematode-destroying fungi by hyphae with clamp connections, a characteristic feature of the Basidiomycotina. Originally the genus could not be linked conclusively with any described fungi possessing sexually reproducing structures (*3*). However, one isolate of *Nematoctonus* from soil subsequently produced fruit bodies of a gilled mushroom (*Hohenbuehelia* sp.) in culture (*4*). Species of *Hohenbuehelia* are found on soil or plant debris but are more commonly associated with rotting wood (*5*).

Rotting wood is a nitrogen-poor environment, as are many bogs. In the early stages of decay the ratio of carbon to available nitrogen is high, and C:N ratios from 350:1 to 1250:1 have been found in sound wood (*6*). Several mechanisms have been suggested by which wood-decay fungi may overcome high C:N ratios. Some of the primary colonizers of dead wood, including *Armillariella mellea* (the honey mushroom), quickly take advantage of sites of high nitrogen concentration such as the cambium, inner bark, and ray cells (*7*). Some of the polypores which penetrate huge volumes of wood conserve the nitrogen obtained by translocating their cytoplasm into the actively growing hyphae (*6*). Shigo (*8*) and others have suggested that the succession of wood-inhabiting microorganisms, including nitrogen-fixing bacteria, may play a role in increasing the amount of nitrogen available to decay fungi. It has been shown that the nitrogen content of wood increases as decay progresses (*9*), but nitrogen may still be limiting because of intense microbial competition. The ability of a *Hohenbuehelia* to capture nematodes suggested a novel means by which wood-rotting fungi could overcome the nitrogen limitations of their primary substrate.

The purpose of our study was to determine the extent and ability of lignicolous gilled fungi to attack and digest nematodes. Twenty-seven species of gilled fungi (Agaricales) were tested for their ability to attack nematodes (Table 1). Pure cultures of the fungi were maintained on potato dextrose agar and incubated at room temperature (18° to 22°C). Methods used to culture nematodes were similar to those described earlier (*2*). To evaluate the nematode-destroying capability of the fungi, a 6-mm disk of each species was transferred to the center of a water agar petri plate and incubated for 7 to 14 days, by which time a thin weft of sparse hyphal growth had radiated from the disk through the adjacent agar. Ten to fifteen active nematodes were handpicked from a nematode culture and placed on the water agar plates in the vicinity of the hyphal growth.

Observations on interactions between nematode and fungus were made immediately and at 15-minute intervals for the first hour, then hourly for the next 12 hours, and again after 24 hours. At daily intervals additional nematodes were added to the culture. The observations were repeated over a period of 7 days.

Of the 27 species tested (Table 1), we found that five species of *Hohenbuehelia*, five species of *Pleurotus*, and one species of *Resupinatus* were capable of destroying nematodes. None of the other fungi had any adverse effects. Nematodes were attacked in one of three different ways.

1) In cultures of *Pleurotus ostreatus* (the oyster mushroom), nematodes be-